Nuclear Science and Techniques (2025) 36:159
https://doi.org/10.1007/s41365-025-01697-1

Solution of multigroup neutron diffusion equation in 3D hexagonal geometry using nodal Green's function method

Il-Mun Ho[1] · Kum-Hyok Ok[1] · Chol So[1]

Received: 18 March 2024 / Revised: 22 May 2024 / Accepted: 1 July 2024 / Published online: 27 June 2025

Abstract
In this paper, we propose a numerical calculation model of the multigroup neutron diffusion equation in 3D hexagonal geometry using the nodal Green's function method and verified it. We obtained one-dimensional transverse integrated equations using the transverse integration procedure over 3D hexagonal geometry and denoted the solutions as a nodal Green's functions under the Neumann boundary condition. By applying a quadratic polynomial expansion of the transverse-averaged quantities, we derived the net neutron current coupling equation, equation for the expansion coefficients of the transverse-averaged neutron flux, and formulas for the coefficient matrix of these equations. We formulated the closed system of equations in correspondence with the boundary conditions. The proposed model was tested by comparing it with the benchmark for the VVER-440 reactor, and the numerical results were in good agreement with the reference solutions.

Keywords NGFM · Hexagonal geometry · Multigroup neutron diffusion equation

1 Introduction

Among the pressurized water reactors (PWRs) operating worldwide, Russian-type PWRs such as VVER-440 and VVER-1000 comprise hexagonal fuel assemblies. Liquid metal fast breeder reactors and very high-temperature reactors under the Next-Generation Nuclear Plant project also use hexagonal assemblies. In addition, these reactors are employed for broader applications in the nuclear industry, such as plutonium and hydrogen production; therefore, considerable improvements have been achieved in the underlying physics calculations of reactors with hexagonal geometry. In the early years, reactor physics calculations for a hexagonal geometry were performed using the finite difference method [1, 2]. In the 1990s, conformal mapping of a hexagon onto a rectangle was reported and codes based on conformal mapping, such as ANC-H [3] and PANTHER [4], were developed. Moreover, numerical methods based on the finite element method have been proposed to solve the neutron diffusion equation for hexagonal geometries [5–8]. The nodal methods developed in the mid-1970s were introduced to neutron diffusion calculations in hexagonal geometry, and nodal method codes such as DIF3D [9] were developed and applied. Owing to the geometrical complexity, it is difficult to solve nodal equations in hexagonal geometry using Cartesian coordinates; therefore, various approximation methods are applied. In the function expansion nodal method (FENM), the neutron flux within a node is expanded using polynomials or exponential functions [10–12]. This method has been used to solve multigroup neutron space-dependent kinetics equations in some studies [13–17]. In Cartesian geometry, nodal methods apply the transverse integration procedure (TIP) to the 3D neutron diffusion equation, resulting in three one-dimensional diffusion equations called transverse integrated equations. When TIP is applied to a hexagonal geometry, singular (discontinuous) terms arise in the transverse leakage terms. Wagner [18] ignored these discontinuous terms in their solution and used lower-order polynomials to approximate the average source of a transverse integrated equation. The use of the nodal Green's function method (NGFM) allows for more accurate treatment of discontinuous terms that arise from the TIP. However, the accurate treatment of discontinuous terms was not implemented in earlier studies [19, 20]. The method presented in [21] improved the accuracy and fidelity of the code by adding the effect of discontinuous terms to the transverse

✉ Il-Mun Ho
im.ho1112@ryongnamsan.edu.kp

[1] Faculty of Energy Science, Kim Il Sung University, Pyongyang, Democratic People's Republic of Korea

integrated flux solution; however, the detailed description was limited to a two-dimensional geometry. In this paper, we propose a numerical model to solve the multigroup neutron diffusion equation in 3D hexagonal geometry using NGFM under the Neumann boundary condition. This model considers discontinuous terms in the solution of the 1D transverse integrated equation. By comparing this with the benchmark for the VVER-440 reactor, we demonstrate the accuracy of the proposed model.

2 Description of the method

2.1 The TIP for multigroup neutron diffusion equation in 3D hexagonal geometry

In 3D Cartesian coordinates (Fig. 1), the multigroup neutron diffusion equation within node k can be written as

$$-D_g^k\left(\frac{\partial^2}{\partial x^2}+\frac{\partial^2}{\partial y^2}+\frac{\partial^2}{\partial z^2}\right)\Phi_g^k(x,y,z)+\Sigma_{r,g}^k\Phi_g^k(x,y,z)=Q_g^k(x,y,z) \tag{1}$$

where

$$Q_g^k(x,y,z)=\left[\sum_{g'\neq g}\Sigma_{g'\to g}^k+\frac{\chi_g}{k_{\text{eff}}}\sum_{g'=1}^{G}\nu\Sigma_{f,g'}^k\right]\Phi_{g'}^k(x,y,z) \tag{2}$$

Integrating Eq. (1) over the volume of node k leads to the following nodal balance equation:

$$\frac{1}{3a}\sum_{x=x,u,v}[J_{gx}^k(a)-J_{gx}^k(-a)]+\frac{1}{2a_z^k}[J_{gz}^k(a_z^k)-J_{gz}^k(-a_z^k)]+\Sigma_{r,g}^k\overline{\Phi}_g^k=\overline{Q}_g^k \tag{3}$$

where

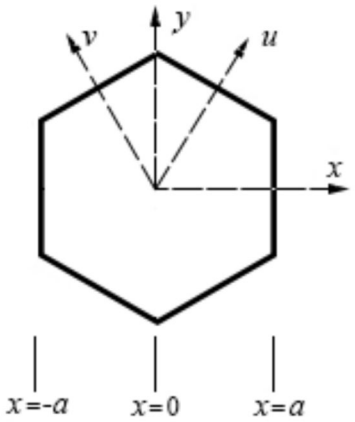

Fig. 1 Hexagonal coordinate system

$$\overline{\Phi}_g^k=\frac{1}{V_k}\int_{-a_z^k}^{a_z^k}\mathrm{d}z\int_{-a}^{a}\mathrm{d}x\int_{-y_s(x)}^{y_s(x)}\Phi_g^k(x,y,z)\mathrm{d}y \tag{4}$$

$$\overline{Q}_g^k=\frac{1}{V_k}\int_{-a_z^k}^{a_z^k}\mathrm{d}z\int_{-a}^{a}\mathrm{d}x\int_{-y_s(x)}^{y_s(x)}Q_g^k(x,y,z)\mathrm{d}y$$
$$V_k=\int_{-a_z^k}^{a_z^k}\mathrm{d}z\int_{-a}^{a}\mathrm{d}x\int_{-y_s(x)}^{y_s(x)}\mathrm{d}y=4\sqrt{3}a^2a_z^k \tag{5}$$

$$y_s(x)=\frac{1}{\sqrt{3}}(2a-|x|) \tag{6}$$

where V_k is the volume of node k; $\overline{\Phi}_g^k$ and $\overline{Q}_g^k$ are the neutron flux and neutron source averaged over V_k, respectively; a is the lattice half pitch; and a_z^k is the haft height of node k.

In Eq. (3),

$$J_{gx}^k(\pm a)=\frac{1}{2a_z^k}\int_{-a_z^k}^{a_z^k}\mathrm{d}z\cdot\left[\frac{1}{2y_s(x)}\int_{-y_s(x)}^{y_s(x)}\left(-D_g^k\frac{\partial}{\partial x}\Phi_g^k(x,y,z)\right)\mathrm{d}y\right]_{x=\pm a} \tag{7}$$

and

$$J_{gz}^k(\pm a_z^k)=\frac{1}{2\sqrt{3}a^2}\int_{-a}^{a}\mathrm{d}x\left[\int_{-y_s(x)}^{y_s(x)}\left(-D_g^k\frac{\partial}{\partial z}\Phi_g^k(x,y,z)\right)\mathrm{d}y\right]_{z=\pm a_z^k} \tag{8}$$

are the net neutron currents averaged at both surfaces in the $x(x=x,u,v)$ and z-directions, respectively.

The transverse integration procedure for Eq. (1) leads to the following equation:

$$-D_g^k\frac{\mathrm{d}^2}{\mathrm{d}x^2}\Phi_{gx}^k(x)+\Sigma_{r,g}^k\Phi_{gx}^k(x)=Q_{gx}^k(x)-L_{gx}^k(x),x(x=x,u,v) \tag{9}$$

where

$$\Phi_{gx}^k(x)=\int_{-a_z^k}^{a_z^k}\mathrm{d}z\int_{-y_s(x)}^{y_s(x)}\Phi_g^k(x,y,z)\mathrm{d}y \tag{10}$$

$$Q_{gx}^k(x)=\int_{-a_z^k}^{a_z^k}\mathrm{d}z\int_{-y_s(x)}^{y_s(x)}Q_g^k(x,y,z)\mathrm{d}y \tag{11}$$

and

$$J_{gx}^k(x)=\int_{-a_z^k}^{a_z^k}\mathrm{d}z\int_{-y_s(x)}^{y_s(x)}\left[-D_g^k\frac{\partial}{\partial x}\Phi_g^k(x,y,z)\right]\mathrm{d}y \tag{12}$$

are the transverse integrated neutron flux, transverse integrated neutron source, and transverse integrated neutron current, respectively. L^k_{gx} is the transverse leakage given by

$$\begin{aligned} L^k_{gx}(x) =& \frac{2}{\sqrt{3}}\left[J^k_{gn}(x,y_s(x)) - J^k_{gn}(x,-y_s(x))\right] \\ &+ J^k_{gz}(x,a^k_z) - J^k_{gz}(x,-a^k_z) \\ &- D^k_g \frac{sgn(x)}{\sqrt{3}}\frac{d}{dx}\left[\boldsymbol{\Phi}^k_g(x,y_s(x)) + \boldsymbol{\Phi}^k_g(x,-y_s(x))\right] \\ &- D^k_g \frac{2\delta(x)}{\sqrt{3}}\left[\boldsymbol{\Phi}^k_g(x,y_s(x)) + \boldsymbol{\Phi}^k_g(x,-y_s(x))\right] \end{aligned} \tag{13}$$

Here, the following relationship between the transverse integrated flux and transverse integrated current is used:

$$\begin{aligned} J^k_{gx}(x) =& -D^k_g \frac{\mathrm{d}}{\mathrm{d}x}\boldsymbol{\Phi}^k_{gx}(x) \\ &+ D^k_g y'_s(x)\left[\boldsymbol{\Phi}^k_g(x,y_s(x)) + \boldsymbol{\Phi}^k_g(x,-y_s(x))\right] \end{aligned} \tag{14}$$

In Eq. (13)

$$\boldsymbol{\Phi}^k_g(x,\pm y_s(x)) = \int_{-a^k_z}^{a^k_z} \boldsymbol{\Phi}^k_g(x,y,z)|_{y=\pm y_s(x)}\mathrm{d}z \tag{15}$$

$$J^k_{gz}(x,\pm a^k_z) = \int_{-y_s(x)}^{y_s(x)} \left[-D^k_g \frac{\partial}{\partial z}\boldsymbol{\Phi}^k_g(x,y,z)\right]_{z=\pm a^k_z}\mathrm{d}y \tag{16}$$

$$J^k_{gn}(x,\pm y_s(x)) = \int_{-a^k_z}^{a^k_z} \left[-D^k_g \frac{\partial}{\partial n}\boldsymbol{\Phi}^k_g(x,y,z)\right]_{y=\pm y_s(x)}\mathrm{d}z \tag{17}$$

and $y'_s(x) = -\frac{1}{\sqrt{3}}sgn(x), y''_s(x) = -\frac{2}{\sqrt{3}}\delta(x)$.

Similar to Eq. (9), the transverse integrated equation along the z-direction is given by

$$-D^k_g \frac{\mathrm{d}^2}{\mathrm{d}z^2}\boldsymbol{\Phi}^k_{gz}(z) + \Sigma^k_{r,g}\boldsymbol{\Phi}^k_{gz}(z) = Q^k_{gz}(z) - L^k_{gz}(z) \tag{18}$$

where

$$\boldsymbol{\Phi}^k_{gz}(z) = \int_{-a}^{a}\mathrm{d}x\int_{-y_s(x)}^{y_s(x)}\boldsymbol{\Phi}^k_g(x,y,z)\mathrm{d}y \tag{19}$$

$$Q^k_{gz}(z) = \int_{-a}^{a}\mathrm{d}x\int_{-y_s(x)}^{y_s(x)}Q^k_g(x,y,z)\mathrm{d}y \tag{20}$$

$$L^k_{gz}(z) = \sum_{x=x,u,v}\left(J^k_{gx}(a,z) - J^k_{gx}(-a,z)\right) \tag{21}$$

$$J^k_{gx}(\pm a,z) = \left[\int_{-y_s(x)}^{y_s(x)}\left(-D^k_g\frac{\partial}{\partial x}\boldsymbol{\Phi}^k_g(x,y,z)\right)\mathrm{d}y\right]_{x=\pm a} \tag{22}$$

We define the transverse-averaged neutron flux, transverse-averaged neutron current, and transverse-averaged neutron source as follows:

$$\overline{\boldsymbol{\Phi}}^k_{gx}(x) = \frac{1}{4y_s(x)a^k_z}\int_{-a^k_z}^{a^k_z}\mathrm{d}z\int_{-y_s(x)}^{y_s(x)}\boldsymbol{\Phi}^k_g(x,y,z)\mathrm{d}y = \frac{1}{4y_s(x)a^k_z}\boldsymbol{\Phi}^k_{gx}(x) \tag{23}$$

$$\begin{aligned} \overline{J}^k_{gx}(x) =& \frac{1}{4y_s(x)a^k_z}\int_{-a^k_z}^{a^k_z}\mathrm{d}z\int_{-y_s(x)}^{y_s(x)}\left[-D^k_g\frac{\partial}{\partial x}\boldsymbol{\Phi}^k_g(x,y,z)\right] \\ &\mathrm{d}y = \frac{1}{4y_s(x)a^k_z}J^k_{gx}(x) \end{aligned} \tag{24}$$

$$\overline{Q}^k_{gx}(x) = \frac{1}{4y_s(x)a^k_z}\int_{-a^k_z}^{a^k_z}\mathrm{d}z\int_{-y_s(x)}^{y_s(x)}Q^k_g(x,y,z)\mathrm{d}y = \frac{1}{4y_s(x)a^k_z}Q^k_{gx}(x) \tag{25}$$

$$\overline{\boldsymbol{\Phi}}^k_{gz}(z) = \frac{1}{2\sqrt{3}a^2}\int_{-a}^{a}\mathrm{d}x\int_{-y_s(x)}^{y_s(x)}\boldsymbol{\Phi}^k_g(x,y,z)\mathrm{d}y = \frac{1}{2\sqrt{3}a^2}\boldsymbol{\Phi}^k_{gz}(z) \tag{26}$$

$$\overline{Q}^k_{gz}(z) = \frac{1}{2\sqrt{3}a^2}\int_{-a}^{a}\mathrm{d}x\int_{-y_s(x)}^{y_s(x)}Q^k_g(x,y,z)\mathrm{d}y = \frac{1}{2\sqrt{3}a^2}Q^k_{gz}(z) \tag{27}$$

Substituting Eqs. (23)–(27) into Eqs. (9) and (18), the following equations for the transverse-averaged neutron fluxes are obtained

$$\begin{aligned} -D^k_g\frac{\mathrm{d}^2}{\mathrm{d}x^2}\overline{\boldsymbol{\Phi}}^k_{gx}(x) + \Sigma^k_{r,g}\overline{\boldsymbol{\Phi}}^k_{gx}(x) &= \overline{Q}^k_{gx}(x) - \overline{L}^k_{gx}(x) \\ &, x(x=x,u,v) \end{aligned} \tag{28}$$

$$-D^k_g\frac{\mathrm{d}^2}{\mathrm{d}z^2}\overline{\boldsymbol{\Phi}}^k_{gz}(z) + \Sigma^k_{r,g}\overline{\boldsymbol{\Phi}}^k_{gz}(z) = \overline{Q}^k_{gz}(z) - \overline{L}^k_{gz}(z) \tag{29}$$

where

$$\begin{aligned} \overline{L}^k_{gx}(x) =& \frac{1}{\sqrt{3}y_s(x)}\left[\overline{J}^k_{gn}(x,y_s(x)) - \overline{J}^k_{gn}(x,-y_s(x))\right] \\ &+ \frac{1}{2a^k_z}\left[\overline{J}^k_{gz}(x,a^k_z) - \overline{J}^k_{gz}(x,-a^k_z)\right] \\ &- D^k_g\frac{sgn(x)}{2\sqrt{3}y_s(x)}\frac{d}{dx}\left[\overline{\boldsymbol{\Phi}}^k_g(x,y_s(x)) + \overline{\boldsymbol{\Phi}}^k_g(x,-y_s(x)) - 4\overline{\boldsymbol{\Phi}}^k_{gx}(x)\right] \\ &- D^k_g\frac{sgn(x)}{2\sqrt{3}y_s(x)}\left[\overline{\boldsymbol{\Phi}}^k_g(x,y_s(x)) + \overline{\boldsymbol{\Phi}}^k_g(x,-y_s(x)) - 2\overline{\boldsymbol{\Phi}}^k_{gx}(x)\right] \end{aligned} \tag{30}$$

$$\bar{L}^k_{gz}(z) = \frac{1}{3a}\sum_{x=x,u,v}\left[\bar{J}^k_{gx}(a,z) - \bar{J}^k_{gx}(-a,z)\right] \tag{31}$$

are the transverse-averaged leakages along the $x(x = x, u, v)$ and z-directions, respectively, and

$$\begin{aligned}
\bar{\Phi}^k_g(x,\pm y_s(x)) &= \frac{1}{2a_z}\Phi^k_g(x,\pm y_s(x)),\\
\bar{J}^k_{gn}(x,\pm y_s(x)) &= \frac{1}{2a_z}J^k_{gn}(x,\pm y_s(x)),\\
\bar{J}^k_{gz}(x,\pm a^k_z) &= \frac{1}{2y_s(x)}J^k_{gz}(x,\pm a^k_z),\\
\bar{J}^k_{gx}(\pm a,z) &= \left[\frac{1}{2y_s(x)}\int_{-y_s(x)}^{y_s(x)}\left(-D^k_g\frac{\partial}{\partial x}\Phi^k_g(x,y,z)\right)\mathrm{d}y\right]
\end{aligned} \tag{32}$$

2.2 Solution to the transverse integrated equation using Green's function under the Neumann boundary condition

Equation (28) is written as follows (the index g and k and the—symbol are omitted for convenience):

$$-D\frac{\mathrm{d}^2}{\mathrm{d}x^2}\Phi(x) + \Sigma_r\Phi(x) = Q(x) - L(x), x = x, u, v \tag{33}$$

The Green's function is the solution of the following equation, which corresponds to Eq. (33)

$$-D\frac{\mathrm{d}^2}{\mathrm{d}x^2}G(x,x_0) + \Sigma_r G(x,x_0) = \delta(x-x_0) \tag{34}$$

Using Neumann boundary conditions, $\left[\frac{\mathrm{d}G(x,x_0)}{\mathrm{d}x}\right]_{x_0=\pm a}$ and Eqs.(14),(23), and (24), the following equation for the transverse-averaged flux is obtained

$$\begin{aligned}
\Phi(x) = &\int_{-a}^{a}(Q(x_0) - L(x_0))G(x,x_0)\mathrm{d}x_0 - J_x(a)G(x,a)\\
&+ J_x(-a)G(x,-a) - \frac{D}{2a}[\Phi_1 + \Phi_2 - 2\Phi_x(a)]G(x,a)\\
&+ \frac{D}{2a}[\Phi_4 + \Phi_5 - 2\Phi_x(-a)]G(x,-a)
\end{aligned} \tag{35}$$

where

$$\begin{aligned}
&\Phi_1 = \Phi(a, y_s(a)), \Phi_2 = \Phi(a, y_s(a)), \text{and}\\
&\Phi_3 = \Phi(0, -y_s(0)), \Phi_4 = \Phi(-a, -y_s(a)),\\
&\Phi_5 = \Phi(-a, y_s(a)), \Phi_6 = \Phi(0, y_s(0))
\end{aligned}$$

are the corner point flux values of the hexagonal node.

We denote the transverse leakage by the sum of the individual terms as follows:

$$L(x) = L_{J,y}(x) + L_{J,z}(x) + L_{\mathrm{sgn}}(x) + L_{\delta}(x) \tag{36}$$

where

$$\begin{aligned}
L_{J,y}(x) &= \frac{1}{\sqrt{3}y_s(x)}[J_n(x,y_s(x)) - J_n(x,-y_s(x))],\\
L_{J,z}(x) &= \frac{1}{2a_z}[J_z(x,a_z) - J_z(x,-a_z)],\\
L_{\mathrm{sgn}}(x) &= -D\frac{sgn(x)}{2\sqrt{3}y_s(x)}\frac{d}{dx}[\Phi(x,y_s(x)) + \Phi(x,-y_s(x)) - 4\Phi(x)],\\
L_{\delta(x)} &= -D\frac{\delta x}{\sqrt{3}y_s(x)}[\Phi(x,y_s(x)) + \Phi(x,-y_s(x)) - 2\Phi(x)],
\end{aligned} \tag{37}$$

where $L_{\mathrm{sgn}}(x)$ and $L_{\delta(x)}$ are the singular (discontinuous) terms that appear in the hexagonal geometry.

Using the following linear approximations for $\Phi(x), \Phi(x, y_s(x)), \Phi(x, -y_s(x))$

$$\Phi(x) = \frac{\Phi(x,y_s(x)) + \Phi(x,-y_s(x))}{2} \tag{38}$$

$$\Phi(x,y_s(x)) = \begin{cases}\dfrac{\Phi_1 - \Phi_6}{a}x + \Phi_6 & x > 0\\ \dfrac{\Phi_5 - \Phi_6}{a}x + \Phi_6 & x < 0\end{cases} \tag{39}$$

$$\Phi(x,-y_s(x)) = \begin{cases}\dfrac{\Phi_2 - \Phi_3}{a}x + \Phi_3, & x > 0\\ \dfrac{\Phi_3 - \Phi_4}{a}x + \Phi_3, & x < 0\end{cases} \tag{40}$$

in Eq.(35), the integral for the discontinuous terms leads to the following equation

$$\begin{aligned}
\Phi(x) = &\int_{-a}^{a}(Q(x_0) - L_J(x_0))G(x,x_0)\mathrm{d}x_0 - J_x(a)G(x,a) + J_x(-a)G(x,-a)\\
&- \frac{D}{2a}[\Phi_1 + \Phi_2 - 2\Phi_x(a)]G(x,a) + \frac{D}{2a}[\Phi_4 + \Phi_5 - 2\Phi_x(-a)]G(x,-a)\\
&+ \frac{D}{2a}[\Phi_3 + \Phi_6 - 2\Phi_x(0)]G(x,0) + \frac{D}{2a}(\Phi_3 + \Phi_6 - \Phi_1 - \Phi_2)\int_0^a\frac{G(x,x_0)}{(2a - x_0)}\mathrm{d}x_0\\
&+ \frac{D}{2a}(\Phi_3 + \Phi_6 - \Phi_4 - \Phi_5)\int_{-a}^{0}\frac{G(x,x_0)}{(2a + x_0)}\mathrm{d}x_0
\end{aligned} \tag{41}$$

where $L_J(x) = L_{J,y}(x) + L_{J,z}(x)$ denotes the practical leakage term in the y and z-directions.

Substituting Eqs. (38), (39) and (40) again into Eq. (41), the fourth, fifth, and sixth terms in right side of Eq. (41) become zero, and thus, the following equation for the transverse-averaged flux is obtained:

$$\begin{aligned}\boldsymbol{\Phi}(x) = &\int_{-a}^{a}(Q(x_0) - L_J(x_0))G(x,x_0)\mathrm{d}x_0 - J_x(a)G(x,a) + J_x(-a)G(x,-a)\\ &+ \frac{D}{2a}(\boldsymbol{\Phi}_3 + \boldsymbol{\Phi}_6 - \boldsymbol{\Phi}_1 - \boldsymbol{\Phi}_2)\int_0^a \frac{G(x,x_0)}{(2a-x_0)}\mathrm{d}x_0 + \frac{D}{2a}(\boldsymbol{\Phi}_3 + \boldsymbol{\Phi}_6 - \boldsymbol{\Phi}_4 - \boldsymbol{\Phi}_5)\int_{-a}^{0}\frac{G(x,x_0)}{(2a+x_0)}\mathrm{d}x_0\end{aligned} \tag{42}$$

2.3 Constitution of the closed system of equations

The transverse-averaged flux, source, and leakage terms are expanded using orthogonal polynomials:

$$\begin{aligned}\boldsymbol{\Phi}(x) &= \sum_{n=0}^{n=2}\boldsymbol{\Phi}_n\omega_n(x)\\ Q(x) &= \sum_{n=0}^{n=2}Q_n\omega_n(x)\\ L_J(x) &= \sum_{n=0}^{n=2}L_n\omega_n(x)\end{aligned} \tag{43}$$

where

$$\omega_0(x) = 1, \omega_1(x) = 3\sqrt{\frac{2}{5}}\frac{x}{a}, \omega_2(x) = \sqrt{\frac{20}{127}}\left(\frac{9x^2}{a^2} - \frac{5}{2}\right) \tag{44}$$

are orthogonal [18]:

$$\frac{1}{2\sqrt{3}a^2}\int_{-a}^{a}2y_s(x)\omega_m(x)\omega_n(x)\mathrm{d}x = \delta_{mn} \tag{45}$$

where $\int_{-a}^{a}dx\int_{-y_s(x)}^{y_s(x)}dy = \int_{-a}^{a}2y_s(x)dx = 2\sqrt{3}a^2$ denotes the area of a hexagon with lattice pitch $2a$.

From Eq. (45), the expansion coefficients in Eq. (43) are given by

$$\begin{aligned}\boldsymbol{\Phi}_n &= \frac{1}{2\sqrt{3}a^2}\int_{-a}^{a}2y_s(x)\boldsymbol{\Phi}(x)\omega_n(x)\mathrm{d}x\\ Q_n &= \frac{1}{2\sqrt{3}a^2}\int_{-a}^{a}2y_s(x)Q(x)\omega_n(x)\mathrm{d}x\end{aligned} \tag{46}$$

$$L_n = \frac{1}{2\sqrt{3}a^2}\int_{-a}^{a}2y_s(x)L(x)\omega_n(x)\mathrm{d}x \tag{47}$$

where Q_n is related to $\boldsymbol{\Phi}_n$ via Eq. (2).

The zeroth-order moment of the transverse-averaged flux equals the node-averaged flux, that is,

$$\begin{aligned}\boldsymbol{\Phi}_0 &= \frac{1}{2\sqrt{3}a^2}\int_{-a}^{a}2y_s(x)\boldsymbol{\Phi}(x)\omega_0(x)\mathrm{d}x\\ &= \frac{1}{2\sqrt{3}a^2}\int_{-a}^{a}2y_s(x)\boldsymbol{\Phi}(x)\mathrm{d}x = \overline{\boldsymbol{\Phi}}\end{aligned} \tag{48}$$

By contrast, the zeroth-order moments of the leakage terms in the y and z coordinate directions are given by

$$\begin{aligned}L_{J,y_0} &= \frac{1}{2\sqrt{3}a^2}\int_{-a}^{a}2y_s(x)L_{J,y}(x)\mathrm{d}x\\ &= \frac{1}{3a}\sum_{s=u,v}[J_s(a) - J_s(-a)] = \overline{L}_{J,y}\end{aligned} \tag{49}$$

$$\begin{aligned}L_{J,z_0} &= \frac{1}{2\sqrt{3}a^2}\int_{-a}^{a}2y_s(x)L_{J,z}(x)\mathrm{d}x\\ &= \frac{1}{3a}\sum_{s=u,v}[J_z(a_z) - J_z(-a_z)] = \overline{L}_{J,z}\end{aligned} \tag{50}$$

The first- and second-order moments can be obtained using an extrapolation procedure for two adjacent nodes, as in a square node.

The transverse-averaged flux at the boundary $x = \pm a$ is as follows:

$$\begin{aligned}\boldsymbol{\Phi}(\pm a) = &\int_{-a}^{a}(Q(x_0) - L_J(x_0)G(x_0,\pm a)\mathrm{d}x_0\\ &- J_x(a)G(a,\pm a) + J_x(-a)G(-a,\pm a)\\ &+ \frac{D}{2a}(\boldsymbol{\Phi}_3 + \boldsymbol{\Phi}_6 - \boldsymbol{\Phi}_1 - \boldsymbol{\Phi}_2)\int_0^a\frac{G(x_0,\pm a)}{2a-x_0}\mathrm{d}x_0\\ &+ \frac{D}{2a}(\boldsymbol{\Phi}_3 + \boldsymbol{\Phi}_6 - \boldsymbol{\Phi}_4 - \boldsymbol{\Phi}_5)\int_{-a}^{0}\frac{G(x_0,\pm a)}{2a+x_0}\mathrm{d}x_0\end{aligned} \tag{51}$$

Inserting Eq. (43) for $Q(x_0)$ and $L_J(x_0)$ into Eq. (51) leads to the following equation

$$\boldsymbol{\Phi}(a) = [G_I+] - J_x(a)G(a,a) + J_x(-a)G(-a,a) + [G_S+] \tag{52}$$

$$\begin{aligned}\boldsymbol{\Phi}(-a) &= [G_I-] - J_x(a)G(a,-a) + J_x(-a)G(-a,-a) \\ &\quad + [G_S-]\end{aligned} \tag{53}$$

where

$$= \sum_{n=0}^{2}(Q_n - L_n)[G_I^{\pm}]_n \tag{54}$$

$$\begin{aligned}[G_S\pm] &= \frac{D}{2a}(\boldsymbol{\Phi}_3 + \boldsymbol{\Phi}_6 - \boldsymbol{\Phi}_1 - \boldsymbol{\Phi}_2)\int_0^a \frac{G(x,\pm a)}{(2a-x)}\mathrm{d}x + \frac{D}{2a}(\boldsymbol{\Phi}_3 + \boldsymbol{\Phi}_6 - \boldsymbol{\Phi}_4 - \boldsymbol{\Phi}_5)\int_{-a}^0 \frac{G(x,\pm a)}{(2a+x)}\mathrm{d}x \\ &= \frac{1}{2a\kappa\sinh 2\kappa a}\left[(\boldsymbol{\Phi}_3 + \boldsymbol{\Phi}_6 - \boldsymbol{\Phi}_1 - \boldsymbol{\Phi}_2)\int_0^a \frac{\cosh\kappa(a\pm x)}{(2a-x)}\mathrm{d}x + \frac{D}{2a}(\boldsymbol{\Phi}_3 + \boldsymbol{\Phi}_6 - \boldsymbol{\Phi}_4 - \boldsymbol{\Phi}_5)\int_{-a}^0 \frac{\cosh\kappa(a\pm x)}{2a+x}\mathrm{d}x\right]\end{aligned} \tag{55}$$

$$\begin{aligned}[G_I^{\pm}]_n &= \int_{-a}^a \omega_n(x)G(x,\pm a)\mathrm{d}x \\ &= \frac{1}{\kappa D\sinh 2\kappa a}\int_{-a}^a \omega_n(x)\cosh\kappa(a\pm x)\mathrm{d}x, \\ &\quad n = 0,1,2\end{aligned} \tag{56}$$

where $\kappa = \sqrt{\frac{\Sigma_r}{D}}$.

Using the continuity conditions of the transverse-averaged flux and the neutron current at the interfaces between adjacent nodes,

$$f_+^k\boldsymbol{\Phi}^k(a) = f_-^{k+1}\boldsymbol{\Phi}^{k+1}(-a) \tag{57}$$

$$J^k(-a) = J^{k-1}(a), J^{k+1}(-a) = J^k(a), \tag{58}$$

the net neutron current coupling equation can be rewritten as

$$\begin{aligned}[G_I^{\pm}]_n &= \int_{-a}^a \omega_n(x)G(x,\pm a)\mathrm{d}x \\ &= \frac{1}{\kappa D\sinh 2\kappa a}\int_{-a}^a \omega_n(x)\cosh\kappa(a\pm x)\mathrm{d}x, \\ &\quad n = 0,1,2\end{aligned} \tag{59}$$

where f_+^k and f_-^{k+1} are the discontinuity factors on the right boundary of node k and left boundary of node $k+1$, respectively. Moreover, $R^k = G^k(a,a), T^k = G^k(a,-a)$ are called the reflective and transmission factors, respectively.

We substitute Eq. (43) into Eq. (42) and multiply both sides of Eq. (42) by $\omega_m(x)$. Using $\frac{2y_s(x)}{2\sqrt{3}a^2}$ as the weighting function and integrating over the interval $[-a,a]$, the following equation for the expansion coefficients of the transverse-averaged flux is obtained:

$$\begin{aligned}\boldsymbol{\Phi} =& [G](Q-L) + [G+]J(a) + [G-]J(-a) \\ &+ \frac{D}{2a}(\boldsymbol{\Phi}_3 + \boldsymbol{\Phi}_6 - \boldsymbol{\Phi}_1 - \boldsymbol{\Phi}_2)[G_{IS}+] \\ &+ \frac{D}{2a}(\boldsymbol{\Phi}_3 + \boldsymbol{\Phi}_6 - \boldsymbol{\Phi}_4 - \boldsymbol{\Phi}_5)[G_{IS}-]\end{aligned} \tag{60}$$

where $[G]$ denotes a 3×3 matrix with the following elements:

$$\begin{aligned}[G]_{mn} &= \frac{1}{2\sqrt{3}a^2}\int_{-a}^a 2y_s(x)\omega_m(x)\mathrm{d}x\int_{-a}^a \omega_n(x_0)G(x,x_0)\mathrm{d}x_0 \\ &= \frac{1}{3a^2}\int_{-a}^a (2a-|x|)\omega_m(x)\mathrm{d}x\left[\int_{-a}^x \omega_n(x_0)\frac{\cosh\kappa(a-x)\cosh\kappa(a+x_0)}{\kappa D\sinh 2\kappa a}\mathrm{d}x_0\right. \\ &\quad \left.+\int_x^a \omega_n(x_0)\frac{\cosh\kappa(a+x)\cosh\kappa(a-x_0)}{\kappa D\sinh 2\kappa a}\mathrm{d}x_0\right], m,n = 0,1,2\end{aligned} \tag{61}$$

The elements of the column vectors $[G\pm]$ and $[G_{IS}\pm]$ are as follows:

$$[G\pm]_n = \frac{1}{2\sqrt{3}a^2}\int_{-a}^{a} 2y_s(x)\omega_n(x)G(x,\pm a)dx = \frac{1}{3a^2\kappa D\sinh 2\kappa a}\int_{-a}^{a}(2a-|x|)\omega_n(x)\cosh\kappa(a\pm x)dx, n=0,1,2 \tag{62}$$

where Φ_i and $\Phi_{i'}(i=1,2,3)$ are the node- and surface-averaged fluxes, respectively.

Note that the corner point numbers in Eqs. (55) and (60) correspond to the calculation along the x-direction. The corner point numbers in the u- and v-directions are

$$\begin{aligned}[G_{IS}+]_n &= \frac{1}{2\sqrt{3}a^2}\int_{-a}^{a}2y_s(x)\omega_n(x)\int_0^a\frac{G(x,x_0)}{2a-x_0}\mathrm{d}x_0\\ &= \frac{1}{3a^2\kappa D\sinh 2\kappa a}\int_0^a\frac{1}{2a-x_0}\mathrm{d}x_0\Big[\cosh\kappa(a-x_0)\int_{-a}^{0}(2a+x)\omega_n(x)\cosh\kappa(a+x)\mathrm{d}x\\ &+\cosh\kappa(a-x_0)\int_0^{x_0}(2a-x)\omega_n(x)\cosh\kappa(a+x)\mathrm{d}x\\ &+\cosh\kappa(a+x_0)\int_{x_0}^{a}(2a-x)\omega_n(x)\cosh\kappa(a-x)\mathrm{d}x\Big], n=0,1,2\end{aligned} \tag{63}$$

$$\begin{aligned}[G_{IS}-]_n &= \frac{1}{2\sqrt{3}a^2}\int_{-a}^{a}2y_s(x)\omega_n(x)\int_{-a}^{0}\frac{G(x,x_0)}{2a+x_0}\mathrm{d}x_0\\ &= \frac{1}{3a^2\kappa D\sinh 2\kappa a}\int_{-a}^{0}\frac{1}{2a+x_0}dx_0\Big[\cosh\kappa(a-x_0)\int_{-a}^{x_0}(2a+x)\omega_n(x)\cosh\kappa(a+x)\mathrm{d}x\\ &+\cosh\kappa(a+x_0)\int_{x_0}^{0}(2a+x)\omega_n(x)\cosh\kappa(a-x)\mathrm{d}x\\ &+\cosh\kappa(a+x_0)\int_0^{a}(2a-x)\omega_n(x)\cosh\kappa(a-x)\mathrm{d}x\Big], n=0,1,2\end{aligned} \tag{64}$$

By contrast, the corner point flux values of a hexagonal node are included in Eqs. (55) and (60), which are also unknown quantities. For the interior nodes away from the reactor core boundaries, we approximate the corner point flux in terms of the node-averaged fluxes, surface-averaged fluxes, and diffusion coefficients in three adjacent nodes, as follows [21]:

$$\Phi_0 = \Big[2(D_1+D_2)\Phi_{1'}+2(D_2+D_3)\Phi_{2'}+2(D_3+D_1)\Phi_{3'} - \sum_{i=1}^{3}D_i\Phi_i\Big]\Big/3(D_1+D_2+D_3) \tag{65}$$

smaller than one and two, respectively, compared to those in the x-direction, that is,

$u-$ axis direction;

$\Phi_1\to\Phi_6, \Phi_2\to\Phi_1, \Phi_3\to\Phi_2, \Phi_4\to\Phi_3, \Phi_5\to\Phi_4, \Phi_6\to\Phi_5$

$v-$ axis direction;

$\Phi_1\to\Phi_5, \Phi_2\to\Phi_6, \Phi_3\to\Phi_1, \Phi_4\to\Phi_2, \Phi_5\to\Phi_3, \Phi_6\to\Phi_4$

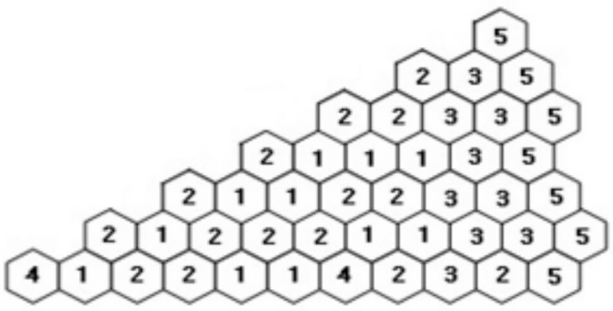

Fig. 2 Material layout of the twelfth core in the VVER-440 problem

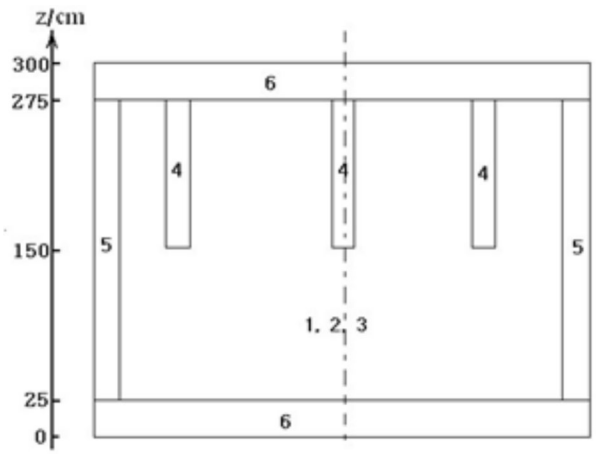

Fig. 3 Material layout on the vertical section of the core

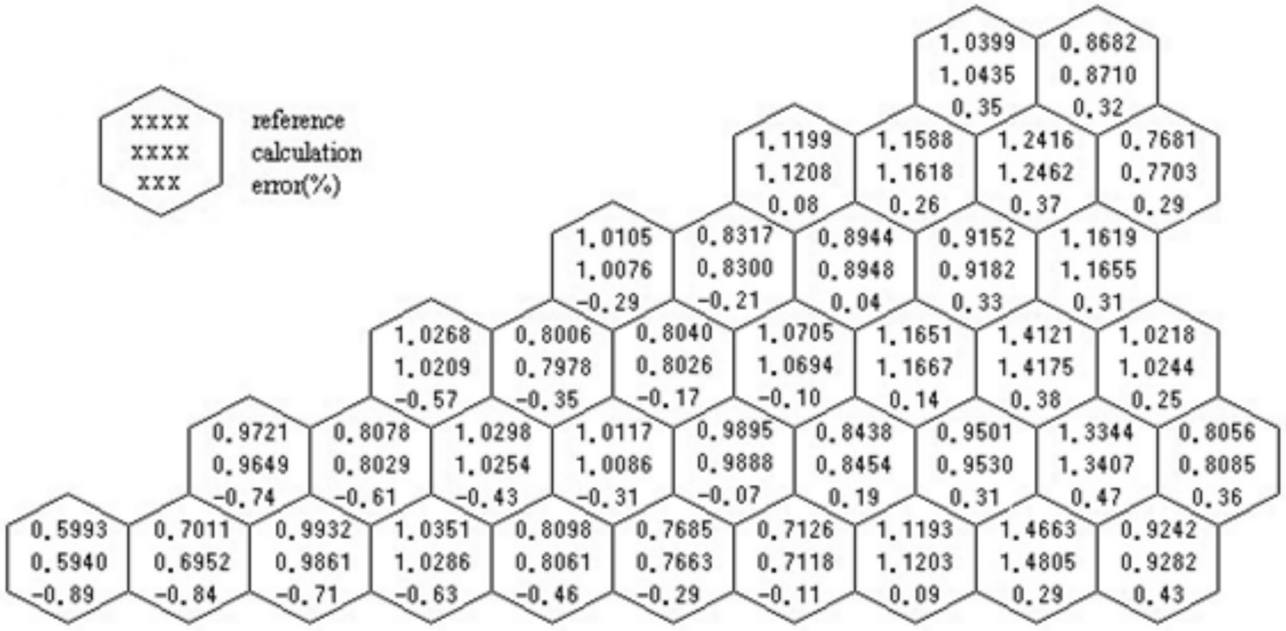

Fig. 4 Assembly-wise normalized power distribution of the twelfth core in the VVER-440 problem

Table 1 Group constants of the materials in the VVER-440 problem

Material	D_1 (cm)	D_2 (cm)	Σ_{r1} (cm^{-1})	Σ_{a2} (cm^{-1})	$\nu\Sigma_{f1}$ (cm^{-1})	$\nu\Sigma_{f2}$ (cm^{-1})	$\Sigma_{1\to2}$ (cm^{-1})
1	1.34660	0.37169	0.025255	0.064277	0.0044488	0.073753	0.016893
2	1.33770	0.36918	0.024709	0.079361	0.0055337	0.105810	0.015912
3	1.33220	0.36502	0.024350	0.10010	0.0070391	0.149640	0.014888
4	1.19530	0.19313	0.035636	0.13498	0.0	0.0	0.022264
5	1.44850	0.25176	0.033184	0.032839	0.0	0.0	0.032262
6	1.34130	0.24871	0.029301	0.064655	0.0	0.0	0.027148

Table 2 Numerical results of the VVER-440 problem

Method	Δk_{eff} (%)	$\Delta P_{\max}$ (%)	ΔP_{avg} (%)
NGFM	0.029	2.51	0.63
FENM	0.026	2.35	0.58
AFEN	0.030	3.20	0.73
ANC-H	0.025	1.28	–

Next, we consider the equation for the transverse-averaged flux in the z-direction

$$-D\frac{\mathrm{d}^2}{\mathrm{d}z^2}\Phi(z)+\Sigma_r\Phi(z)=Q(z)-L(z) \tag{66}$$

In this case, there are no discontinuous terms in the transverse leakage; therefore, the procedure is similar to that for a square node [22–24]. In addition, Legendre polynomials are used instead of Eq. (44). Then, the zeroth-order moment of the transverse leakage term becomes

$$\begin{aligned} L_{z0}=\frac{1}{a_z}\int_{-a_z}^{a_z}L(z)\mathrm{d}z=\frac{1}{3a}\sum_{s=x,u,v}\frac{1}{2a_z}\int_{-a_z}^{a_z}\left\{\left[\frac{1}{2y_s(x)}\int_{-y_s(x)}^{y_s(x)}\left(-D\frac{\partial}{\partial x}\Phi(x,y,z)\right)\mathrm{d}y\right]_{x=a}\mathrm{d}z\right. \\ \left.-\left[\frac{1}{2y_s(x)}\int_{-y_s(x)}^{y_s(x)}\left(-D\frac{\partial}{\partial x}\Phi(x,y,z)\right)\mathrm{d}y\right]_{x=-a}\mathrm{d}z\right\}=\frac{1}{3a}\sum_{s=x,u,v}[J_s(a)-J_s(-a)]=\bar{L}_z \end{aligned} \tag{67}$$

The first- and second-order moments of the transverse leakage term are the same as those of the square node. The net neutron current coupling equation, equation for the

expansion coefficients of the transverse-averaged flux, and matrix elements included in these equations also have the same forms as those in a square node.

The nodal balance equation, net neutron current coupling equation in each coordinate direction, its boundary conditions, and equation for the expansion coefficients of the transverse-averaged flux constitute a closed system of equations.

3 Numerical results

The three-dimensional VVER-440 benchmark [3] was used to test the proposed numerical method. The material layout of the core of the problem is shown in Figs. 2 and 3. The group constants of these materials are listed in Table 1. The numerical results of this problem are summarized in Table 2, where Δk_{eff} is the error of the effective multiplication factor and ΔP_{max} and ΔP_{avg} are the maximum and average errors of the nodal power, respectively. For comparison, the numerical results of the other methods are also presented in this table. NGFM is the code based on the numerical method proposed in this study, and FENM, AFEN, and ANC-H are the codes based on the flux expansion nodal method, analytic function expansion nodal method, and conformal mapping, respectively, [12]. The accuracy of our numerical results was similar to that of other numerical methods. The effective multiplication factor obtained from our calculation was 1.01161, and the difference from the reference value (1.01132) was 0.029%. The maximum and average percentage errors of the nodal power were 2.51% and 0.63%, respectively. In the calculations, the axial mesh spacing was set to 25 cm. The reference solution was obtained from DIF3D-FD [25] runs with 216 and 294 triangle/hexagon subdivisions and a 2.5-cm axial mesh spacing. Figure 4 shows the assembly-wise normalized power distribution. The maximum error in the assembly-wise normalized power was 0.89%. These results show that the proposed numerical method is accurate for solving neutron diffusion equations in hexagonal-z geometry.

4 Conclusion

A numerical model was proposed to solve the neutron diffusion equation in hexagonal-z geometry, and the discontinuous terms in the transverse leakage were explicitly considered in this model. The solution of 1D transverse integrated equation was expressed using the nodal Green's function under the Neumann boundary condition. Using the quadratic polynomial expansion of the transverse-averaged quantities, the net neutron current coupling equation and equation for the expansion coefficients of the transverse-averaged neutron flux were obtained. We constructed a closed system of equations by deriving the equations corresponding to the boundary conditions. The numerical model proposed in this study was tested by comparison with the benchmark for the VVER-440 reactor, and the numerical results were in good agreement with the reference solutions.

Author Contributions All authors contributed to the study conception and design. Data collection and analysis were performed by Il-Mun Ho, Kum-Hyok Ok and Chol So. The first draft of the manuscript was written by Il-Mun Ho, and all authors commented on previous versions of the manuscript. All authors read and approved the final manuscript.

Declarations

Conflict of interest The authors declare that they have no conflict of interest.

References

1. T.B. Fowler, D.R. Vondy, G.W. Gunningham, Nuclear reactor core analysis code: citation. ORNL-TM-2496 (1971)
2. H. Finnermann, R. Böer, R. Müller, Combination of finite-difference and finite-volume techniques in global reactor calculation. Kerntechnik **57**, 216–222 (1992). https://doi.org/10.1515/kern-1992-570406
3. Y.A. Chao, Y.A. Shatilla, Conformal mapping and hexagonal nodal methods-II, implementation in the ANC-H code. Nucl. Sci. Eng. **121**, 210–225 (1995). https://doi.org/10.13182/nse95-a28559
4. M. Knight, P. Hutt, I. Lewis, Comparison of PANTHER nodal solutions in hexagonal-z geometry. Nucl. Sci. Eng. **121**, 254–263 (1995). https://doi.org/10.13182/nse95-a28562
5. J.J. Lautard, S. Loubiere, C. Fedon-Magnaud, CRONOS: a modular computational system for neutronic core calculations, IAEA-TECDOC-678 (1992)
6. A. Hébert, Application of a dual variational formulation to finite element reactor calculations. Ann. Nucl. Energy **20**, 823–845 (1993). https://doi.org/10.1016/0306-4549(93)90076-2
7. S.G. Pintor, D. Ginestar, G. Verdu, High order finite element method for the lambda modes problem on hexagonal geometry. Ann. Nucl. Energy **36**, 1450–1462 (2009). https://doi.org/10.1016/j.anucene.2009.07.003
8. C.Y. Zhang, G. Chen, Fast solution of neutron transport SP3 equation by reduced basis finite element method. Ann. Nucl. Energy **120**, 707–714 (2018). https://doi.org/10.1016/j.anucene.2018.06.042
9. R.D. Lawrence., The DIF3D nodal neutronics option for two- and three-dimensional diffusion theory calculations in hexagonal geometry. ANL-83-1 (1983). https://doi.org/10.2172/6318594
10. U. Grundmann, F. Hollstein, Two-dimensional intra-nodal flux expansion method for hexagonal geometry. Nucl. Sci. Eng. **133**, 201–212 (1999). https://doi.org/10.13182/NSE99-A2082
11. V.G. Zimin, D.M. Baturin, Polynomial nodal method for solving neutron diffusion equations in hexagonal-z geometry. Ann. Nucl. Energy **29**, 1105–1117 (2002). https://doi.org/10.1016/S0306-4549(01)00083-4
12. B. Xia, Z. Xie, Flux expansion nodal method for solving multigroup neutron diffusion equations in hexagonal-z geometry. Ann. Nucl. Energy **33**, 370–376 (2006). https://doi.org/10.1016/j.anucene.2005.06.011
13. S. Duerigen, U. Rohde, Y. Bilodid et al., The reactor dynamics code DYN3D and its trigonal-geometry nodal diffusion model.

Kerntechnik **78**, 310–318 (2013). https://doi.org/10.3139/124.110382
14. Y. Bilodid, U. Grundmann, S. Kliem, The HEXNEM3 nodal flux expansion method for the hexagonal geometry in the code DYN3D. Ann. Nucl. Energy **116**, 187–194 (2018). https://doi.org/10.1016/j.anucene.2018.02.037
15. Y. Cai, X.J. Peng, W.B. Zhao et al., The numerical solution of space-dependent neutron kinetics equations in hexagonal-z geometry using Diagonally Implicit Runge-Kutta method. Ann. Nucl. Energy **94**, 150–154 (2016). https://doi.org/10.1016/j.anucene.2016.03.006
16. Y. Cai, X.J. Peng, Q. Li et al., The numerical solution of space-dependent neutron kinetics equations in hexagonal-z geometry using backward differentiation formula with adaptive step size. Ann. Nucl. Energy **128**, 203–208 (2019). https://doi.org/10.1016/j.anucene.2019.01.004
17. K. Srebrin, I. Christoskov, A modal ACMFD formulation of the HEXNEM3 method for solving the time-dependent neutron diffusion equation. Ann. Nucl. Energy **130**, 331–337 (2019). https://doi.org/10.1016/j.anucene.2019.03.006
18. M.R. Wagner, Three-dimensional nodal diffusion and transport theory methods for hexagonal-z geometry. Nucl. Sci. Eng. **103**, 377 (1989). https://doi.org/10.13182/nse89-a23690
19. A.M. Ougouag, Systematics of neutron diffusion modeling for neutron-optically thin, multiply-heterogeneous High Temperature Reactors. INL/EXT-09-16414(2009)
20. W. Firzpatrick, Developments in nodal reactor analysis for hexagonal geometry. PhD Thesis Universtity of Illinois at Urbana-Champaign (1995). https://doi.org/10.5555/220627
21. R.M. Ferrer, A.M. Ougouag, A.A. Bingham, Nodal Green's Function Method singular source term and burnable Poison treatment in hexagonal geometry. INL/EXT-09-16773(2009) https://doi.org/10.2172/983357
22. R.D. Lawrence, J.J. Dorning, A nodal Green's function method for multidimensional neutron diffusion calculations. Nucl. Sci. Eng. **76**, 218–231 (1980). https://doi.org/10.13182/NSE80-A19452
23. Y.M. Hu, X.F. Zhao, Advanced nodal Green's function method on Neumann boundary condition. J. Tsinghua Univ. (Sci. Technol.) **38**, 17–21 (1998)
24. I.M. Ho, C. So, Coupled 3D neutron kinetics/thermal-hydraulics calculation of PWR core using nodal Green's function method on Neumann boundary condition. Prog. Nucl. Energy **123**, 103316 (2020). https://doi.org/10.1016/j.pnucene.2020.103316
25. K.L. Derstine, DIF3D: A code to solve one-, two-, and three-dimensional finite-difference diffusion theory problems, ANL-82-64(1984). https://doi.org/10.2172/7157044